

## **Sonochemical Surface Functionalization of Exfoliated LDH: Effect on Textural Properties, CO<sub>2</sub> Adsorption, Cyclic Regeneration Capacities and Subsequent Gas Uptake for Simultaneous Methanol Synthesis**

**Collins I. Ezeh<sup>a</sup>, Huang Xiani<sup>a</sup>, Xiaogang Yang<sup>a,\*</sup>, Cheng-gong Sun<sup>b,\*</sup>, Jiawei Wang**

<sup>a</sup>Department of Mechanical, Materials and Manufacturing Engineering  
University of Nottingham Ningbo  
University Park, Ningbo 315100. P.R. China

<sup>b</sup>Department of Chemical and Environmental Engineering  
University of Nottingham  
University Park, Nottingham NG7 2RD, UK

<sup>c</sup>Chemical Engineering & Applied Chemistry  
School of Engineering and Applied Science  
Aston University  
Birmingham B4 7ET, UK

### **Abstract**

To improve CO<sub>2</sub> adsorption, amine modified Layered double hydroxide (LDHs) were prepared via a two stage process, SDS/APTS intercalation was supported by ultrasonic irradiation and then followed by MEA extraction. The prepared samples were characterised using Scanning electron microscope-Energy dispersive X-ray spectroscopy (SEM-EDX), X-ray Photoelectron Spectroscopy (XPS), X-ray diffraction (XRD), Temperature Programmed Desorption (TPD), Brunauer-Emmett-Teller (BET), and Thermogravimetric analysis (TGA), respectively. The characterisation results were compared with those obtained using the conventional preparation method with consideration to the effect of sonochemical functionalization on textural properties, adsorption capacity, regeneration and lifetime of the LDH adsorbent. It is found that LDHs prepared by sonochemical modification had improved pore structure and CO<sub>2</sub> adsorption capacity, depending on sonic intensity. This is attributed to the enhanced deprotonation of activated amino functional groups via the sonochemical process. Subsequently, this improved the amine loading and effective amine efficiency by 60% of the conventional. In addition, the sonochemical process improved the thermal stability of the adsorbent and also, reduced the irreversible CO<sub>2</sub> uptake, C<sub>Uirrev</sub>, from 0.18 mmol/g to 0.03 mmol/g. Subsequently, improving the lifetime and ease of regenerating the adsorbent respectively. This is authenticated by subjecting the prepared adsorbents to series of thermal swing adsorption (TSA) cycles until its adsorption capacity goes below 60% of the original CO<sub>2</sub> uptake. While the conventional adsorbent underwent a 10 TSA cycles before breaking down, the sonochemically functionalized LDH went further than 30 TSA cycles.

**Keywords:** *CO<sub>2</sub> Capture, Layered Double Hydroxide, Ultrasound, Adsorption, Regeneration.*

---

\*Corresponding authors:

Tel: +86-574-88182419 E-mail: [Xiaogang.Yang@nottingham.edu.cn](mailto:Xiaogang.Yang@nottingham.edu.cn) (X. Yang)

Tel: +44-115-7484577 E-mail: [cheng-gong.sun@nottingham.ac.uk](mailto:cheng-gong.sun@nottingham.ac.uk) (C. Sun)

## 1. INTRODUCTION

Carbon dioxide adsorption is viewed as one of the promising methods in Carbon Capture and Storage (CCS) technology (1, 2). It has been widely accepted that an estimated 30-50% energy requirement reduction can be obtained when compared to absorption by amine solvents (3, 4). However, numerous factors must be considered for achieving this optimum performance as pointed out by Drage et al. (4). Extensive reviews on materials used for CO<sub>2</sub> adsorption have been done by many researchers. These materials include amine polymers (5, 6), immobilized amines (7, 8), carbonaceous materials (9-11), Layered double hydroxides (LDHs) (2, 12, 13), zeolites (14-16) and organic-inorganic hybrids (17-19). Owing to its comparably high adsorption capacity and numerous catalytic applications (13, 20), the LDHs has been broadly investigated and considered to be one of the most promising flexible adsorbents (21). In addition, its ionic inter-layered structural configuration provides the material with relatively high contact surface area and active basic sites to serve as a catalyst (or support) (20). However, the material is challenged by its low CO<sub>2</sub> uptake, regeneration capacity and thermo-stability (21, 22).

The low adsorption capacity of LDH is partly attributed to the poor textural characteristics (23, 24) and low amine loading as reported in previous studies (2). Adopted methods to improve these features involved the use of anionic surfactants and organoalkoxysilane amines which served the purpose of widening the interlayer gallery of the LDHs to bolster its exfoliation process (12) while simultaneously increasing the amine content (25). Frequently used surfactants are sodium dodecyl sulphate (SDS) (2, 26) and sodium dodecyl sulphonate (27), while the organoalkoxysilanes includes N-trimethoxysilylpropyl-N,N,N-trimethylammonium chloride (28), (3-aminopropyl)-triethoxysilane (APTS) (2, 27, 29) and (3-aminopropyl)-trimethoxysilane (ATMS) (26). Nonetheless, reported amine loading and subsequent adsorption capacity of the adsorbent is not satisfactory. This was attributed to the poor pore structure of the adsorbent.(24). To further enhance the porosity and textural properties of the adsorbent, sonic irradiation has been applied in chemical synthesis of the

adsorbent. Ultrasonic technology has been observed to rapidly promote inorganic and organic reactions without weakening the final material properties (23). Furthermore, this technology improves the porosity and surface area of the synthesized material in addition to increasing metallic dispersion across the material (13). However, in its industrial applicability, the prepared adsorbent should be able to withstand the thermal atmosphere during adsorption. Review of sonochemical route reports that ultrasonic irradiation can lead to detrimental acoustic cavitation (30) which can result to breakdown of the material. This can be partly due to the sonic intensity. Another crucial feature of LDH for industrial application is the lifetime and ease of regenerating the adsorbent. The ease of regeneration will reduce the energy required for CO<sub>2</sub> recovery; hence, improving the overall capture efficiency. Moreover, the adsorbents lifetime will define the rate of replacing the adsorbent, consecutively affecting the process economics.

In this work, we have understudied the contribution of the sonochemical preparation of functionalized LDH to its industrial applicability with regards to its textural characteristics, thermal strength, adsorption and cyclic regeneration capacity, as well as its impact for further gaseous adsorption. The LDH adsorbents were synthesised via anionic surfactant interaction and amine extraction through ultrasonic modulation. The adopted amine used for functionalization of the LDH is monoethanolamine (MEA). The obtained LDHs were characterised using Scanning Electron Microscope (SEM), Energy Dispersion X-ray Spectroscopy (EDX), Brunauer-Emmett-Teller (BET), Thermal Gravimetric Analyzer (TGA), Temperature-Programmed Desorption (TPD), X-ray Photoelectron Spectroscopy (XPS) and X-ray Diffraction (XRD). With consideration to the energy demand for CO<sub>2</sub> recovery, transportation and storage, the thermal swing adsorption cycle (TSA) was favoured against the pressure swing adsorption (PSA) to study the cyclic regeneration of the adsorbent (5). To this regard, the regeneration of the adsorbent was carried out isothermally at ambient pressure using N<sub>2</sub> as the stripping gas. The adsorbents lifetime was also examined over numerous TSA cycles till its CO<sub>2</sub> uptake is 60% of the original sorption capacity.

## 2. EXPERIMENTAL

### 2.1. Materials

The LDHs were prepared via different route: co-precipitation and ultrasonic mediated means. Subsequently, MEA extractions of these LDHs were carried out to produce the amine modified LDHs. All reagents used for material synthesis were purchased from SinoPharm Chemical Reagents Co. Ltd. The CO<sub>2</sub> and N<sub>2</sub> gases used for characterization and adsorption measurements are 99.99% pure and were supplied by Linde Group, China.

### 2.2. Sample Synthesis

For *MgAl LDH*, 200 ml solution containing APTS ( $\geq 98\%$ ) and SDS ( $\geq 86\%$ ) (molar ratio: 5:1) respectively dissolved in a mixture of 50 ml C<sub>2</sub>H<sub>5</sub>OH ( $\geq 99.7\%$ ) and 150 ml distilled water was stirred for about 30 min at a temperature of 60 °C until the pH stabilized at about 10.3. This solution was then reacted with Mg(NO<sub>3</sub>)<sub>2</sub>·6H<sub>2</sub>O ( $\geq 98\%$ ) and Al(NO<sub>3</sub>)<sub>3</sub>·9H<sub>2</sub>O ( $\geq 99\%$ ) (molar ratio: 3:1, dissolved in 100 ml of distilled water) solution by adding the latter dropwise while maintaining the temperature of the former at 60 °C. pH of the mixture was regulated towards 10 by adding 4 M NaOH ( $\geq 96\%$ ) solution. The substrate with a molar ratio of Mg:Al:APTS:SDS = 3:1:5:1 was then aged for 20hr with the temperature and stirring maintained. The precipitates were filtered, washed with distilled water and then dried in a vacuum oven (500 mbar at 70 °C) overnight. This sample is labelled as LDH5. Varying the amount of SDS, two other samples were produced with mole ratios of Mg:Al:APTS:SDS = 3:1:5:2.5 and 3:1:5:5 labelled as LDH2 and LDH1 respectively. Using the same chemical composition and process, a set of new samples were prepared using sonicated mixing either by ultrasonic horns (high intensity sonication, 600W) or bath (low intensity sonication, 150W). These samples are labelled as UH-LDH<sub>n</sub> and UB-LDH<sub>n</sub> respectively, n being the stoichiometric ratio of APTS to SDS.

For *MgAl LDH-MEA*, in the preparation of the amine modified LDH, the SDS surfactant were removed via MEA extraction as applied by Zheng et al. (31). 0.5 g of LDH5 sample was

dispersed in a solution of 100ml C<sub>2</sub>H<sub>5</sub>OH ( $\geq 99.7\%$ ) containing 20g MEA ( $\geq 99\%$ ). The mixture was then refluxed for 20 hr at a temperature of 90 °C. After which the samples were filtered, washed with ethanol and dried in a vacuum oven overnight. These samples are labelled LDH-MEA5, LDH-MEA2 and LDH-MEA1 respectively. Using an ultrasonic bath, the procedure was repeated for the synthesised UB-LDHn samples. Synthesised UB-LDHn samples were similarly dispersed in a solution of C<sub>2</sub>H<sub>5</sub>OH and MEA; and then refluxed for 20 hr while using the ultrasonic bath filled with distilled water at a temperature of 90 °C. The obtained samples are labelled as UB-MEAn. In the same procedure, UH-MEAn samples were prepared. During reflux, ultrasonic horn was used rather than the bath.

## **2.3. Characterization**

**2.3.1. Scanning Electron Microscopy (SEM) – Energy Dispersive X-ray Spectroscopy (EDX) Analysis.** The surface morphology of the prepared materials were studied with a Zeiss SIGMA™ Field Emission SEM. With the aid of an Oxford Instrument INCAx-act PentaFET® Precision EDX, the EDX spectra for the LDHs were obtained. This was also used to compute the amine content present in the adsorbents.

**2.3.2. X-ray Diffraction (XRD and X-ray Photoelectron Spectroscopy (XPS)) Analysis.** XRD patterns were studied using a Bruker-AXS D8 advance powder diffractometer with a scanning range of  $10^\circ \leq 2\theta \leq 90^\circ$ . The basal spacing was calculated with Bragg's Law using the  $d_{003}$  peak from the diffraction pattern. X-ray Photoelectron Spectroscopy (XPS) data of the adsorbent was obtained using Kratos X-ray Photoelectron Spectrometer – Axis Ultra DLD with a 96 W monochromatic Al K $\alpha$  X-ray source (1486.69 eV) at a photoelectron take-off angle of 45°. Wide scans were performed from 1100 eV to 0 eV with a dwell time of 150 ms and steps of 1 eV. Narrow scans were performed with steps of 0.05 eV with dwell time of 600 ms. The binding energy (BE) was calibrated by using the C 1s peak at 284.6 eV as a reference.

**2.3.3. Nitrogen Adsorption-Desorption Measurement.** The textural properties of the prepared adsorbents were studied by Nitrogen physisorption analysis at  $-196\text{ }^{\circ}\text{C}$  using the Micrometrics ASAP 2020 Surface Area and Porosity Analyser. Prior to this analysis, samples were degassed at a temperature of  $105\text{ }^{\circ}\text{C}$  for 4hr. The BET (Brunauer, Emmett and Teller) model was used to determine the surface area ( $S_{\text{BET}}$ ) of the samples. The total pore volumes ( $V_{\text{Total}}$ ) were computed from the amount of nitrogen adsorbed at relative pressure ( $P/P_0$ ) of 0.99 and the average pore volumes from  $4V_{\text{Total}}/S_{\text{BET}}$ . The pore size distribution was calculated using the BJH (Barrett, Joyner and Halenda) model. The t-plot method was used to calculate the micropore volume ( $V_{\text{micro}}$ ).

**2.3.4. CO<sub>2</sub> Uptake Measurement.** CO<sub>2</sub> adsorption was measured by a Netzsch STA 449 F3 Jupiter thermo-gravimetric analyser (TGA). Approximately 5-10 mg of each sample was heated from 25 to  $105\text{ }^{\circ}\text{C}$  at  $20\text{ }^{\circ}\text{C}/\text{min}$  under N<sub>2</sub>. The sample was held at  $105\text{ }^{\circ}\text{C}$  for 30 min and then cooled to the desired adsorption temperature at a rate of  $10\text{ }^{\circ}\text{C}/\text{min}$ . The gas input was switched from N<sub>2</sub> to CO<sub>2</sub> and held isothermally for 90 min. The experimented adsorption temperatures were  $55\text{ }^{\circ}\text{C}$  and  $80\text{ }^{\circ}\text{C}$  (reported optimum adsorption temperature for most amine functionalised adsorbents (32)). The CO<sub>2</sub> adsorption capacity was determined from the weight change of the samples in CO<sub>2</sub> atmosphere. Effects of the change in gas density and viscosity were corrected by measuring the response to an empty alumina crucible using the same method.

**2.3.5. Adsorbent Regeneration via Thermal Swing Adsorption Cycles.** A thermal swing adsorption-desorption programme in the presence of N<sub>2</sub> was conducted using the Netzsch STA 449 F3 Jupiter thermo-gravimetric analyser. This is to determine the lifetime adsorption capacity of the adsorbent. After the CO<sub>2</sub> uptake measurement, the adsorbent was heated to  $105\text{ }^{\circ}\text{C}$  at a rate of  $20\text{ }^{\circ}\text{C}/\text{min}$  in a N<sub>2</sub> atmosphere with a constant flow rate of  $20\text{ ml}/\text{min}$  and held isothermally for 30 mins. After desorption, the adsorption cycle was repeated several times. The experimented adsorption temperature is  $55\text{ }^{\circ}\text{C}$ . Adsorption capacities were computed based on the mass of the adsorbent.

**2.3.6. Thermal Stability Measurement.** The stability of the as synthesised LDH samples in air was determined using the Netzsch STA 449 F3 Jupiter thermogravimetric analyser. About 5-10 mg of sample was loaded into an alumina crucible, and the decomposition was monitored by increasing temperature from 25 to 1000 °C with a heating rate of 10 °C/min and under a flow of air (50 ml/min).

### **2.3.7. Temperature-Programmed Desorption (TPD)**

CO<sub>2</sub>-TPD analysis was conducted using AutoChem II 2920. The TPD of CO<sub>2</sub> measurements were implemented to analyze the acidity and basicity of the catalysts. 0.1 g of the adsorbent was first placed in the reactor and treated at 350 °C for 2 hr in N<sub>2</sub>. During desorption, a thermal conductivity detector (TCD) was employed to record the TPD profiles from 100 to 800 °C with a heating rate of 10 °C/min.

## **3. RESULTS AND DISCUSSION**

Figure 1 shows the SEM images of prepared LDHs. At low amount of SDS (Mole ratio,  $n = 5$ ), the layered hydroxide exhibits irregular shapes and is highly porous and permeable with little or no agglomeration on the surface of the sample. As the addition of SDS increases, APTS/SDS mole ratio decreases, accompanied by significant changes of the surface of the adsorbent with remarkably increased particle agglomeration. It can be seen from the figure that the LDH2 sample clearly forms a flake-like shell over an irregular dense shaped core. Further increase of SDS results in the flake-like shell becoming curled up as can be seen from the sample of LDH1. This may be explained by the formation of shell-core structure caused by the sequential reduction of two different metallic ions (33), resulting from difference in the reduction potentials of Mg<sup>2+</sup> and Al<sup>3+</sup> ions. It could be said that the excess Mg<sup>2+</sup> ions are oxidized preferably to the Al<sup>3+</sup> ions, resulting in the formation of Mg-core/Al-shell particles. The increased particle aggregation and subsequent surface restructuring was due to the physiochemical property of SDS. Due to its mean aggregation number of 62, SDS are able to form aggregates at high concentrations (34). Comparing the inter-layer spacing between the flake-shells for different samples, LDH2 seems to be more spaced due to an irregular layering of flakes. Unlike LDH2, LDH1 was observed to have a lower interlayer spacing due to the

folding of the flaky layers while undergoing intra-layer interactions. The amine modified LDHs show similar surface structures irrespective of the variation in SDS amount. However, they exhibited more surface granular agglomeration, as seen from Figure 2. It is interesting to note here that the flaky-shells of the LDH2 and LDH1 were no longer visible after applying MEA extraction. The samples of LDH-MEA2 and LDH-MEA1 showed some coated edges on the surface of the particles while this was not found in the sample of LDH-MEA5. Figure 3 shows the SEM image of LDH prepared using ultrasonic irradiation at APTS/SDS mole ratio of 5 (UH-LDH5) in comparison to the conventional method. The surface of the sonicated LDH shows an evenly distributed undulated surface sites (fig. 3b) when compared to that of the conventional (Fig. 3a). This stresses the impact of the sonication on the morphology, and probably, on the physical properties of the material (33) as shown in the Table 1. Comparing the BET results of the conventional and sonochemically modified LDHs, it is observed that there is a significant difference in the textural properties of LDHs.  $S_{BET}$  and  $V_{Total}$  increased from 25.03 m<sup>2</sup>/g and 0.02 cm<sup>3</sup>/g for the conventional route to 171.20 m<sup>2</sup>/g and 0.5528 cm<sup>3</sup>/g respectively from the sonochemical process. However, the percentage of micropores to the total pore volume showed a decrease in value.

In order to fundamentally reveal the effect of addition of SDS on the internal structures of the LDHs and modified LDHs, the X-ray diffraction (XRD) was also used to characterise the prepared samples. The XRD pattern for LDH samples are shown in Figure 4. A rough look from the figure indicates that all samples exhibit similar patterns. However, a careful observation reveals that the intensity of the reflections at the peaks differs for each sample. A notable peak appears at  $2\theta = 60^\circ$ . The appearance of this peak is as a result of overlapping of reflections from structural configurations of (113) and (110). It has been observed from the test that an increase in SDS (decrease in n) results in a decrease in the non-basal reflections. Reflections at (110) are common for the non-modified LDHs with large interlayer spacing (33, 35). Hence, it can be stipulated that the increase in SDS will result in the reduction of large interlayer spacing (2), supported by the SEM images of the LDHs. Another insignificantly notable variation in peaks was observed to occur at  $15^\circ \leq 2\theta \leq 25^\circ$ . Within this range, the reflection is likely associated with the lattice (0018) (36). It was also noticed that

the increase in surfactant results in an increase in the reflection sharpness and intensity. This clearly indicates that the crystallinity of the sample increases for the LDH modification with SDS-APTS intercalation. However, the non-basal reflections at (012) seem to be preserved, indicating that the layered structures were unaffected by the change in surfactant amount. These trends were also observed in the sonochemically modified LDHs (Figures 5-8). Figures 5 and 6 show the XRD patterns for the sonicated LDH samples using low and high intensity sonications respectively. The patterns show similar trends to those of non-sonicated LDHn. It can be conjectured with a certain reservation that the adoption of sonication has no remarkable impact on the structure of the LDHn. However, a slight increase in the peak of (110) reflection was noticed for both ultrasonic modulated LDH. The use of MEA extraction for all prepared samples also demonstrates less influence on the structure of the adsorbents. The results of non-basal XRD peaks (0018), (012) and (110) shown in Figures 7 and 8 clearly indicates that the structure of the adsorbents is less affected by using MEA extraction.

### **3.2 Effect of amine modification on the prepared LDH on CO<sub>2</sub> adsorption capacity**

For evaluating the effect of amine modification on CO<sub>2</sub> adsorption capacity, the characterisation of CO<sub>2</sub> adsorption process using the TGA is divided into three phases: (1) pre-heating of the sample from room temperature to 105°C for 30 minutes under N<sub>2</sub> atmosphere for the removal of absorbed water molecules; (2) under the same N<sub>2</sub> atmosphere, the sample was then cooled to the desired temperature for adsorption; and (3) switching the gas from N<sub>2</sub> to CO<sub>2</sub> for isothermal CO<sub>2</sub> adsorption. In the third phase, the CO<sub>2</sub> adsorbed by the sample is measured from the weight gained by the sample. An illustration of this process is shown in Figure 9(a).

Figure 10 shows the CO<sub>2</sub> adsorption capacities for those samples of (a) LDHn and (b) LDH-MEAn (with n being the molar ratio of APTS to SDS). The adsorption experiments were carried out twice (Supplementary document, Table S1) and the data of the averaged weight gained from CO<sub>2</sub> adsorption were used in generating the figure. It was observed from the obtained data that as SDS increases (indicated by the decrease in mole ratio from 5 to 1) at 55

°C, the CO<sub>2</sub> uptake decreases from 0.82 to 0.59 mmol/g. This is consistent with finding reported in previous study but with lower CO<sub>2</sub> adsorption capacities 0.58 to 0.12 mmol/g (2). The decrease in adsorption capacity is attributed to the protonation of amino groups by the surfactant's anions given the increased addition of SDS, thus preventing CO<sub>2</sub> adsorption on these sites. The same trend was also observed at 80 °C but with a decreased adsorption capacity of about 35-50% of that at 55 °C.

After adoption of MEA extraction, the CO<sub>2</sub> uptake by the LDH-MEA samples at 55°C increased by about 75-90% based on the LDH samples. This is partly due to the increased amine loading, facilitating the extraction of the surfactant and consequently making the amino groups available for CO<sub>2</sub> adsorption. This trend was also found at 80°C with an increase of about 10-30% in the CO<sub>2</sub> adsorption capacity of the LDH-MEAs. This significant change in adsorption performance can be explained by the CO<sub>2</sub> adsorption profile of APTS at varying temperature which tends to achieve the maximum in the range of the temperature of 60 to 70 °C (2). This trend was also observed in the sonicated LDHs. After amine modification, the adsorption capacity at 55 °C of the UB-LDH5 increased from 0.48 to 0.54 mmol/g, while UH-LDH increased from 0.66 – 1.37 mmol/g (Table 2). This increase can be attributed to the exfoliation of the surfactant and simultaneous increase in the amine loading by the MEA extraction process. In this regard, the interacted amino groups with the negative head-groups of the surfactant are deprotonated, which are now free to react with CO<sub>2</sub>. This can be validated by the increase in amine loading after MEA extraction as shown in Table 2.

Using the EDX spectroscopy, inspection tests were carried out for each LDH and the tabulated results (Table 2) show the average composition of the samples. The EDX results show the elemental configuration and dispersion across the internal micro structures of the prepared samples (Supplementary documents, Figure S1). From the obtained elemental analysis, the molecular formula of the grafted organic species, SDS and APTS, was computed using the general chemical formula for all amine modified LDH,  $[Mg_3Al(OH)_m]_x^+ \cdot [C_{12}H_{25}SO_4]_y^- \cdot [C_nH_{2.5n+0.5}SiNO_3]_z$  (5). From the table, it is observed that the amount of sulphur reduced after MEA extraction resulting to a corresponding increase in nitrogen content. This shows that the extraction process was effective (c.a. 97-99% of SDS

was removed) across all preparation route; hence, increasing the adsorption capacity after MEA extraction.

### **3.3 Effect of ultrasonic modulation on CO<sub>2</sub> adsorption capacity**

The effect of ultrasonic modulation was also studied in the preparation process. The stirring process was sonicated by applying either ultrasonic horn or ultrasonic bath. Table 4 shows the CO<sub>2</sub> uptake by LDHs produced using ultrasonic irradiation with ultrasonic horn and bath at temperatures of 55 °C and 80 °C. The results show a reduction in CO<sub>2</sub> uptake at both temperatures when compared to the conventional co-precipitation route as shown in Figure 11. It should be noted here that the result is yet to be validated with an optimum sonication condition for this material. This is subject to further research. However, the decrease in CO<sub>2</sub> adsorption by the sonicated sample can be explained by the enhanced chemical reaction facilitated by accelerated inter-particle collision within the local hot spot of the collapsing bubbles that are generated by the sonication (33). Consequently, the available amino groups are readily bonded to the anionic surfactants, resulting to limited amino group active site for CO<sub>2</sub> adsorption. Sonication aids in rearranging reactions with a bias towards reaction mechanisms that yields molecules not necessarily obtained from purely thermal or light induced reactions (35) or by adjusted physicochemical parameters (33). Adequate studies must be carried out to discern the optimal ultrasonic power output for any preparation process. This importance can be illustrated by the use of mild sonication using ultrasonic bath rather than intense sonication from the ultrasonic horn. With the limited results obtained from the ultrasonic bath, it was observed that at a temperature of 80 °C, the CO<sub>2</sub> adsorbed at APTS/SDS mole ratio of 5, 2 and 1 are 0.74, 0.81 and 0.61 mmol/g, respectively, which is remarkably higher than that obtainable from the conventional LDHs (0.54, 0.20 and 0.315 mmol/g, respectively) and LDH-MEAs (0.695, 0.22 and 0.40 mmol/g, respectively). This clearly demonstrated that the preparation method can be optimised for favourable adsorbent synthesis using the controlled sonication.

At the given desirable temperature of 55 °C, a comparison of the CO<sub>2</sub> uptake profile by the conventional and ultrasonic irradiation (both horn and bath) for APTS/SDS mole ratio of 5 is

shown in Figure 12. In comparison to the conventional LDH5, the sonochemically prepared adsorbents, UB-LDH5 and UH-LDH5 exhibit a lower CO<sub>2</sub> uptake of 0.44 and 0.66 mmol/g respectively despite the high amine loading of 1.21 and 2.22 mmol/g when compared to the 0.46 mmol/g of the conventional with a CO<sub>2</sub> uptake of 0.82 mmol/g (see Table 2). This can be attributed to the enhanced protonation of the amino groups by the negative head of the surfactant caused by the ultrasonic irradiation irrespective of the high surfactant content in LDH5 (depicted by the high SDS/APTS ratio), which still possesses more active amino groups for CO<sub>2</sub> uptake. This is supported by the XPS result presented in Figure 13. XPS was conducted to investigate the content of the amino functional group on the adsorbent surface. Two bands of N 1s spectrum of LDH were observed at *ca.* 397 eV (Peak 1) and 401 eV (Peak 2) binding energies. These are assigned to free amine and protonated/H-bonded amines respectively (37, 38). The spectrum shows the sonochemically prepared LDH to have less concentration of free amines, depicted by peak 1 (Fig. 13b) when compared to that of the conventional (Fig. 13a). Consequently, it reveals that there are limited amino group active sites readily available for CO<sub>2</sub> adsorption for UH-LDH. . In addition, it is also relevant to note that the amine loading increased with sonication intensity. This is subject to further research for optimizing adsorbent performance. However, after amine modification, the amine loading of LDH-MEA5, UB-MEA5 and UH-MEA5 increased to 4.71, 5.26 and 5.24 mmol/g respectively with a corresponding increase in CO<sub>2</sub> uptake to 1.45, 0.54 and 1.37 mmol/g respectively. As reported by Wang et al (2), the average amine loading for monomeric amines grafted adsorbents is 3-4 mmol/g (See supporting document, S3). However, in this study, it is shown that this can be further improved via ultrasonic irradiation. The incremental change in amine loading is part due to the exfoliation of the surfactant. Nonetheless, the percentage of surfactants removed decreased insignificantly according to the trend conventional>UB>UH. Subsequently, this has an impact on the effective amine loading and effective amine efficiency. In this study, the effective amine efficiency was calculated as the amount of CO<sub>2</sub> uptake resulting from the additional amine loading after LDH functionalization with MEA. UH-MEA5 showed the highest effective amine efficiency of 0.24 compared to 0.15 of LDH-MEA5. This elaborates the importance of sonication in

deprotonating protonated and/or probably dispersing the amino groups during MEA extraction, making these groups available as active sites for CO<sub>2</sub> adsorption by about 60%.

### **3.4 Effect of the preparation routes on thermal stability of the amine modified LDHn**

Using the TGA, the thermal stability of the prepared samples was determined from room temperature of about 20 °C to 1000 °C at a variation rate of 10 °C/min. The TGA profiles, as shown in Figure 14, indicate that the samples disintegrate within three temperature phases:  $T < \sim 150$  °C,  $\sim 150 < T < \sim 750$  °C and  $\sim 750$  °C < T. However, the second stage of disintegration for LDHn shows an uneven weight loss as compared to the regular weight loss for LDH-MEA<sub>n</sub>. The first stage of weight loss ( $T < \sim 150$  °C) is attributed to the loss of interstitial water molecules. While for the second phase ( $\sim 150 < T < \sim 750$  °C), the decomposition can be ascribed to the dehydroxylation and breakdown of the organic alkyl chain of the LDH. The observed irregular decomposition curve in this stage may implicate the occurrence of an uneven bonding structure, resulting to multi-stage dehydroxylation processes. The final weight loss ( $\sim 750$  °C < T) results from the decomposition of the sulphate species residuum.

Table 4 shows the tabulated results of the weight loss (%) of LDHn samples prepared using conventional and the ultrasonic routes. From the table, it can be seen that as the APTS/SDS mole ratio, n, reduces, the amount of interstitial moisture decreases. This has been observed in all preparation methods and could be explained by the additional presence of anionic surfactants that replace the water molecules. However, the ultrasonic route (UH) shows a less weight loss in the second and third stage (49-64%) compared with the UB-route (54-66%), which has a nearly same weight loss as that of the conventional method (54-66%). This can be further elaborated by the comparison of those curves in Figure 14a-c, where the decomposition curves of LDH and UB-LDH are seen to be undulated while the decomposition curve of UH-LDH seems to be regular, likely attributed to the more uniform mixing in UH-LDH so that a more even bonding structure within the material can be obtained. This indicates that the adoption of the UH-route may be beneficial to the synthesis of a more stable material than the UB and the conventional method.

After introducing amine modification of the samples, the decomposition curves clearly show different behaviour compared with that of the untreated LDHs prepared by the different methods. The curves display a well-defined three phase decomposition steps unlike the untreated ones, as can be seen from Figure 14(d-f). Within the same temperature range as that of the LDHs, the MEA-treated LDHs show higher moisture content than the unprocessed ones (See Supporting document, S5). This can be caused by the presence of leftover MEA molecules after the extraction process. However, the weight losses in the second and third phase reduce significantly, benefitting to production of a more stable material than the pure LDH. This can be explained by the reduced presence of the surfactant after the amine extraction.

In addition, it can be discerned that the sonochemically prepared samples (UB-MEA and UH-MEA) demonstrate a more thermally stable profile than the conventional ones, showing by the total weight loss of 46-52% as compared with 53-64% of the LDH-MEA samples. This demonstrates that the adoption of ultrasonic route may contribute to an accessible distribution of the surfactant during the preparation of the LDH. As a result, the surfactants are easily extracted during the MEA extraction process, thus enhancing the stability of prepared material.

### **3.5 Effect of the sonochemical functionalization on ease of regeneration, lifetime of the LDH adsorbent and subsequent gas uptake.**

After CO<sub>2</sub> adsorption, the adsorbents were subjected to a desorption process at a temperature of 105 °C for 30 mins in N<sub>2</sub> atmosphere. This was used to compute the ease of recovering the adsorbed CO<sub>2</sub> within the given regeneration test time. The ease of regeneration will contribute to the overall capture efficiency over a period of time and will impact on the economics of the process. Figure 9(b) shows an example of recoverable CO<sub>2</sub> uptake using TSA. The recoverable CO<sub>2</sub> uptake was denoted as CU<sub>rev</sub>, while the retained CO<sub>2</sub> uptake as CU<sub>irrev</sub>. The results (Table 1) show that the sonochemical functionalized LDHs, UB-MEA5 and UH-MEA5 has CU<sub>rev</sub> of 0.51 and 1.33 mmol/g representing c.a. 93% and 98% of the CO<sub>2</sub> uptake. Compared with the CU<sub>rev</sub> of the conventional modified LDH-MEA5, of 1.27 mmol/g (c.a. 87% of the adsorbed CO<sub>2</sub>), the sonochemically prepared adsorbents showed a

better performance for the capture of CO<sub>2</sub>. Analysing the  $CU_{rev}$  for UH-MEA5 and LDH-MEA5, it is observed that despite the higher CO<sub>2</sub> uptake of LDH-MEA5, the amount of CO<sub>2</sub> recovered during desorption is lower than that of UH-MEA5.

The impact of the preparation route on the cyclic sorption capacity is presented in Figure 14. The sorption capacity is calculated as a percentage of the original capacity of 1.45 and 1.37 mmol/g for LDH-MEA5 and UH-MEA5 respectively. These two adsorbents were considered given that they have close adsorption capacities and that UH-MEA5 was more stable than UB-MEA5. The TSA cycle was repeated several times, with a regeneration temperature of 105 °C until the sorption capacity reduced below 60% of the original capacity. For deployment of these adsorbents on a large scale, the greater the cyclic adsorption capacity, the lesser the replacement of the adsorbent and potentially more efficient the adsorbent will be. From Figure 15, LDH-MEA5 showed an initial high cyclic adsorption capacity greater than 90% of the initial sorption capacity. However, its lifetime did not exceed the 11<sup>th</sup> cycle before degrading to a capacity less than 60% of the original sorption uptake. Degradation in cyclic adsorption capacity can be attributed to the secondary reaction occurring between the amino group and CO<sub>2</sub> as observed in Figure 12 (b). This is shown by the second ascent in CO<sub>2</sub> uptake after 48, 50 and 55 mins of adsorption by LDH-MEA5, UB-MEA5 and UH-MEA5 respectively. Drage et al. (5) refuted the possibility of adsorbent volatilization or loss of reactive amino functional groups as the responsible factors for degradation in performance of amine grafted adsorbent. It was revealed that secondary reaction resulted in the formation of stable poly urea compounds deposited on the adsorbent. This corresponds to the 12.64%, 6.39% and 2.43% of  $CU_{irrev}$  for LDH-MEA5, UB-MEA5 and UH-MEA5 respectively (Table 1) elaborating the potential ease of formation of urea linkages in the conventional LDH adsorbent. These linkages pose a deleterious effect on the reaction between CO<sub>2</sub> and the active amino functional groups. The destructive impact of this side reaction can be a contributor to the breakdown of LDH-MEA5 under numerous TSA cycles especially when the adsorption cycle is increased beyond 60 mins. Unlike the LDH-MEA5, UH-MEA5 displayed a lower initial cyclic adsorption capacity (averaging about 80%) but seemed to oscillate about this capacity for more than 30 TSA cycles (triple the lifetime of LDH-MEA5).

These hypotheses can be supported by CO<sub>2</sub>-TPD profile on the functionalised LDH is shown in Figure 16. The desorption of CO<sub>2</sub> occurs at overlapping peaks of 270 °C ( $\alpha$ ) and 363 °C ( $\beta$ ), 474 °C ( $\gamma$ ) and 569 °C ( $\delta$ ) (Figure 16a). The  $\alpha$ -peak has been assigned to CO<sub>2</sub> desorption from bicarbonates formed on OH- groups and tends to occur at low temperatures, whereas the  $\beta$ -peak occurs at intermediate temperatures and is characterised by desorption of CO<sub>2</sub> from bidentate carbonates formed on metal-oxygen pairs. At high temperatures, desorption is attributed to monodentate carbonates produced on low-coordination oxygen anions (23). This is designated by the  $\gamma$  and  $\delta$ -peaks (22). In this study, the low and intermediate energy states are the major contributors to CO<sub>2</sub> uptake, predominated by the intermediate energy state. This is more pronounced in the ultrasonic irradiated adsorbents as shown in Figure 16b where intermediate energy desorption of UH-MEA5 outweighs that of LDH-MEA5. Nonetheless, the reverse was observed at low energy desorption with LDH-MEA5 slightly desorbing more CO<sub>2</sub> than UH-MEA5. However, the overall desorption by the sonochemically prepared LDH within the time analysed showed a better performance than the conventional. In other words, it can be deduced that the performance of a conventionally synthesised LDH is dependent on its basicity while sonochemically synthesised LDHs will profit from low regeneration temperature gradients, especially in temperature-swing operations.

These findings were further compared to pseudo-first and pseudo-second order kinetic models:

Pseudo-first order:

$$\text{Equation: } x = A_1(1 - e^{-k_1 t}); \quad \text{Differential form: } \frac{dx}{dt} = k_1(A_1 - x)$$

Pseudo-second order:

$$\text{Equation: } x = \frac{A_2^2 k_2 t}{A_2 k_2 t + 1}; \quad \text{Differential form: } \frac{dx}{dt} = k_2(A_2 - x)^2$$

where  $x$  and  $A_i$ ,  $i=1, 2$  represents the CO<sub>2</sub> uptake at a given time and equilibrium respectively for an  $i^{\text{th}}$  order model,  $k_i$ ,  $i=1, 2$  is the  $i^{\text{th}}$  order rate constant and  $t$  is the time of adsorption. The obtained experimental data are fitted to the models and selecting the one with the best fit. To

determine the suitability of each model, an error function (Err) defined by Equation 1 was applied:

$$Err (\%) = \sqrt{\frac{\sum \left[ \frac{(x_{exp} - x_{mod})}{x_{exp}} \right]^2}{N - 1}} \times 100 \quad (1)$$

where  $x_{exp}$  and  $x_{mod}$  are CO<sub>2</sub> uptake determined experimentally and computed using the model respectively and N is the total number of experimental points. It is reasonable to assume that the adsorption rate constant, k for both pseudo-first and -second order model is the same for each group of functionalized and non-functionalized adsorbents since they are both grafted with the same amino silane. The kinetic parameters are shown in Table 5 with the estimated standard errors and R<sup>2</sup> values. From the simulation results, it is observed that pseudo-second order model displayed a comparatively good fit with the value of equilibrium CO<sub>2</sub> uptake close to that of experimental data for the non-functionalized adsorbents. Hence, despite the effect of sonication on the adsorption capacity and textural properties of the adsorbent, the adsorption kinetics is more favoured by the second order rate function. This model explains adsorption process involving chemical reactions or at high amine loading as compared to pseudo-first order model which explains adsorption under low surface coverage. However, after amine extraction, UH-MEA5 experimental data was best fitted by the pseudo-first order model with a standard error of 0.20%. This explains the ease of recovering the CO<sub>2</sub> uptake as a result of the minimal chemisorption. Figure 15 shows the fitting of the models with the experimental data for conventional (LDH5) and sonicated (UH-LDH5) non-functionalized adsorbents. Despite the pseudo second order being the better fit, the standard error tends to increase in the sonication route.

After CO<sub>2</sub> adsorption by the LDH adsorbent, the adsorbents were subjected to further isothermal adsorption in N<sub>2</sub> atmosphere at 50 ml/min for 20 mins. This is to measure the additional gas uptake capacity of the adsorbent when considered as a catalytic support for hydrogenation of the adsorbed CO<sub>2</sub> to methanol. From the results (Table 1), it is observed that the ultrasonic mediated adsorbents (UB-MEA5 and UH-MEA5) showed a greater potential for additional gaseous uptake than the conventional LDH-MEA5. The amount of N<sub>2</sub>

adsorbed per adsorbed CO<sub>2</sub> were 0.31, 0.25 and 0.16 mmol N<sub>2</sub>/mmol CO<sub>2</sub> for UH-MEA5, UB-MEA5 and LDH-MEA5 respectively. This can be attributed to the high pore volume of the sonochemically produced adsorbents. Hence, proposing the sonochemical process as a viable catalyst preparation means for synthesising methanol via hydrogenation of CO<sub>2</sub>.

#### **4. Conclusions**

The present study has shown that the LDHs with high CO<sub>2</sub> adsorption capacity can be synthesised via amine modification by means of anionic surfactant intercalation reinforced by ultrasonic irradiation. The use of sonochemical process in the synthesis step led to a more developed pore structure than that of the conventional process. However, this was dependent on sonication intensity. Despite the advancement in physical properties which is beneficial to the physical adsorption of CO<sub>2</sub>, the further adoption of the sonochemical process for amine functionalization of the prepared LDH led to an improved amine loading and effective amine efficiency of the adsorbent. In addition, the recoverable CO<sub>2</sub> uptake of the sonochemically prepared adsorbent increased to 1.33 mmol/g as against 1.27 mmol/g of the conventional. In combination with the improved thermal stability of the adsorbent as a result of this process, the sonochemically functionalized LDH exhibited a greater ease of regeneration with a longer life span than the conventional LDH. Therefore, sonochemical route can be an effective preparation method for long-lasting recyclable layered double hydroxides for CO<sub>2</sub> adsorption.

#### **ACKNOWLEDGEMENT**

This work was carried out at the International Doctoral Innovation Centre (IDIC). The authors would like to acknowledge the financial support through the grants of the Zhejiang Provincial Natural Science Foundation (Grant No. LY15B06000) and Ningbo Key Research Project 'Absorption/catalytic technologies for the simultaneous removal of multi-pollutants from flue gas at power stations' (Grant No. 1012B10042), and from Ningbo Education Bureau, Ningbo Science and Technology Bureau, China's MoST and The University of Nottingham. The work is also partially supported by EPSRC (Grant no. EP/G037345/1).

## References

1. Figueroa JD, Fout T, Plasynski S, McIlvried H, Srivastava RD. Advances in CO<sub>2</sub> capture technology—The U.S. Department of Energy's Carbon Sequestration Program. *International Journal of Greenhouse Gas Control*. 2008;2(1):9-20.
2. Wang J, Stevens LA, Drage TC, Snape CE, Wood J. Preparation and CO<sub>2</sub> adsorption of amine modified layered double hydroxide via anionic surfactant-mediated route. *Chemical Engineering Journal*. 2012;181-182:267-75.
3. Gray ML, Champagne KJ, Fauth D, Baltrus JP, Pennline H. Performance of immobilized tertiary amine solid sorbents for the capture of carbon dioxide. *International Journal of Greenhouse Gas Control*. 2008;2(1):3-8.
4. Drage TC, Snape CE, Stevens LA, Wood J, Wang J, Cooper AI, et al. Materials challenges for the development of solid sorbents for post-combustion carbon capture. *Journal of Materials Chemistry*. 2012;22(7):2815.
5. Drage TC, Arenillas A, Smith KM, Snape CE. Thermal stability of polyethylenimine based carbon dioxide adsorbents and its influence on selection of regeneration strategies. *Microporous and Mesoporous Materials*. 2008;116(1-3):504-12.
6. Xu X, Song C, Andréßen JM, Miller BG, Scaroni AW. Preparation and characterization of novel CO<sub>2</sub> “molecular basket” adsorbents based on polymer-modified mesoporous molecular sieve MCM-41. *Microporous and Mesoporous Materials*. 2003;62(1-2):29-45.
7. Tanthana J, Chuang SS. In situ infrared study of the role of PEG in stabilizing silica-supported amines for CO<sub>2</sub> capture. *ChemSusChem*. 2010;3(8):957-64.
8. Serna-Guerrero R, Da'na E, Sayari A. New Insights into the Interactions of CO<sub>2</sub> with Amine-Functionalized Silica. *Industrial and Engineering Chemistry Research*. 2008;47(23):9406-12.
9. Saha D, Deng S. Adsorption equilibrium and kinetics of CO<sub>2</sub>, CH<sub>4</sub>, N<sub>2</sub>O, and NH<sub>3</sub> on ordered mesoporous carbon. *Journal of colloid and interface science*. 2010;345(2):402-9.
10. Cinke M, Li J, Bauschlicher CW, Ricca A, Meyyappan M. CO<sub>2</sub> adsorption in single-walled carbon nanotubes. *Chemical Physics Letters*. 2003;376(5-6):761-6.
11. Arenillas A, Smith KM, Drage TC, Snape CE. CO<sub>2</sub> capture using some fly ash-derived carbon materials. *Fuel*. 2005;84(17):2204-10.
12. Park A-Y, Kwon H, Woo AJ, Kim S-J. Layered Double Hydroxide Surface Modified with (3-Aminopropyl)triethoxysilane by Covalent Bonding. *Advanced Materials*. 2005;17(1):106-9.
13. Szabados M, Mészáros R, Erdei S, Kónya Z, Kukovecz Á, Sipos P, et al. Ultrasonically-enhanced mechanochemical synthesis of CaAl-layered double hydroxides intercalated by a variety of inorganic anions. *Ultrasonics Sonochemistry*. 2016;31:409-16.
14. Hernandez-Huesca R, Diaz L, Aguilar-Armenta G. Adsorption Equilibria and Kinetics of CO<sub>2</sub>, CH<sub>4</sub> and N<sub>2</sub> in Natural Zeolites. *Separation and Purification Technology*. 1999;15:163-73.
15. Siriwardane RV, Shen M-S, Fisher EP. Adsorption of CO<sub>2</sub> on Zeolites at Moderate Temperatures. *Energy & Fuels*. 2005;19:1153-9.

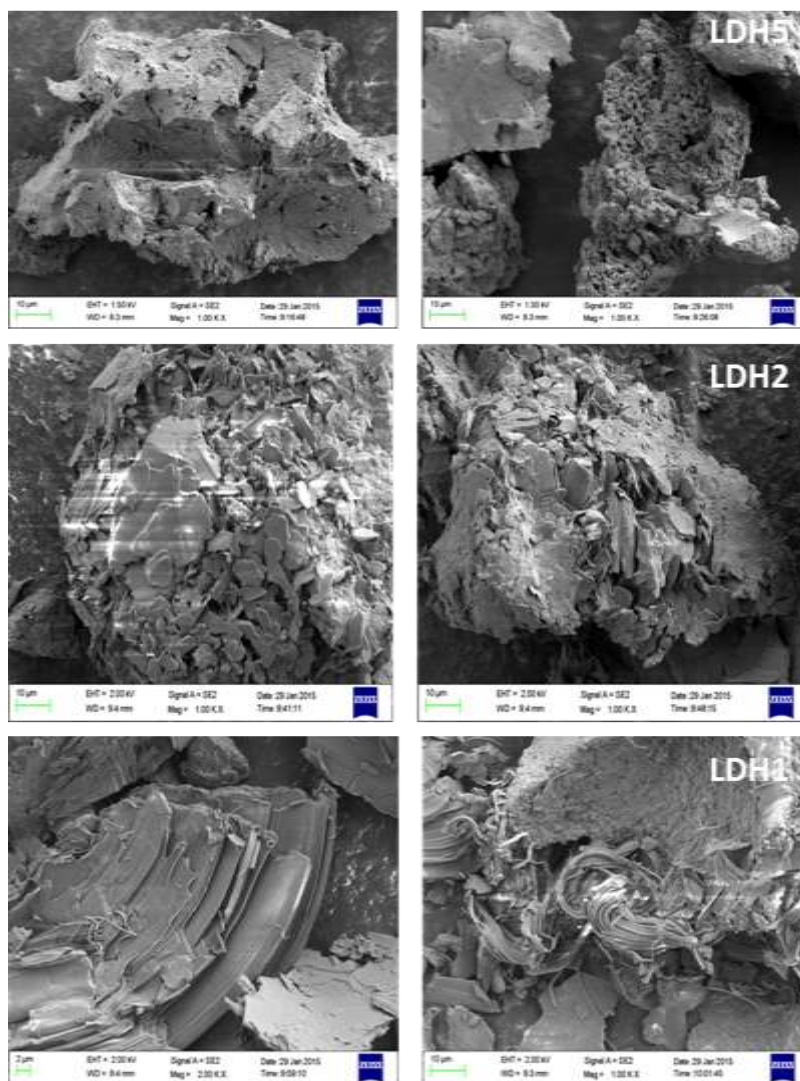
16. Walton KS, Abney MB, Douglas LeVan M. CO<sub>2</sub> adsorption in Y and X zeolites modified by alkali metal cation exchange. *Microporous and Mesoporous Materials*. 2006;91(1-3):78-84.
17. Bae Y-S, Farha OK, Hupp JT, Snurr RQ. Enhancement of CO<sub>2</sub>/N<sub>2</sub> selectivity in a metal-organic framework by cavity modification. *Journal of Materials Chemistry*. 2009;19(15):2131.
18. Yang D-A, Cho H-Y, Kim J, Yang S-T, Ahn W-S. CO<sub>2</sub> capture and conversion using Mg-MOF-74 prepared by a sonochemical method. *Energy & Environmental Science*. 2012;5(4):6465.
19. Yamamoto K, Sakata Y, Nohara Y, Takahashi Y, Tatsumi T. Organic-inorganic hybrid zeolites containing organic frameworks. *Science*. 2003;300:470-2.
20. Cavani F, Trifirò F, Vaccari A. Hydrotalcite-type anionic clays: Preparation, properties and applications. *Catalysis Today*. 1991;11(2):173-301.
21. Wang Q, Luo J, Zhong Z, Borgna A. CO<sub>2</sub> Capture by Solid Adsorbents and their Applications: Current Status and New Trends. *Energy & Environmental Science*. 2011;4(1):42.
22. Ferrer DI. Supported Layered Double Hydroxides as CO<sub>2</sub> Adsorbents for Sorption-enhanced H<sub>2</sub> Production. Springer International Publishing Switzerland: Imperial College, London, United Kingdom; 2016.
23. Zhao S, Yi H, Tang X, Gao F, Yu Q, Zhou Y, et al. Enhancement effects of ultrasound assisted in the synthesis of NiAl hydrotalcite for carbonyl sulfide removal. *Ultrasonics Sonochemistry*. 2016;32:336-42.
24. Bernardo MP, Moreira FKV, Colnago LA, Ribeiro C. Physico-chemical assessment of [Mg-Al-PO<sub>4</sub>]-LDHs obtained by structural reconstruction in high concentration of phosphate. *Colloids and Surfaces A: Physicochemical and Engineering Aspects*. 2016;497:53-62.
25. Kenarsari SD, Yang D, Jiang G, Zhang S, Wang J, Russell AG, et al. Review of recent advances in carbon dioxide separation and capture. *RSC Advances*. 2013;3(45):22739.
26. Yao K, Imai Y, Shi L, Dong A, Adachi Y, Nishikubo K, et al. The functional layered organosilica materials prepared with anion surfactant templates. *Journal of colloid and interface science*. 2005;285(1):259-66.
27. Tao Q, He H, Frost RL, Yuan P, Zhu J. Nanomaterials based upon silylated layered double hydroxides. *Applied Surface Science*. 2009;255(7):4334-40.
28. Che S, Garcia-Bennett AE, Yokoi T, Sakamoto K, Kunieda H, Terasaki O, et al. A novel anionic surfactant templating route for synthesizing mesoporous silica with unique structure. *Nat Mater*. 2003;2(12):801-5.
29. Yokoi T, Yoshitake H, Tatsumi T. Synthesis of Anionic-Surfactant-Templated Mesoporous Silica using Organoalkoxysilane-containing Amino Groups. *Chemistry of Materials*. 2003;15(24):4536-8.
30. Xu H, Zeiger BW, Suslick KS. Sonochemical synthesis of nanomaterials. *Chemical Society reviews*. 2013;42:2555-67.
31. Zheng H, Gao C, Che S. Amino and quaternary ammonium group functionalized mesoporous silica: An efficient ion-exchange method to remove anionic surfactant from AMS. *Microporous and Mesoporous Materials*. 2008;116(1-3):299-307.

32. Zhao X, Hu X, Hu G, Bai R, Dai W, Fan M, et al. Enhancement of CO<sub>2</sub> adsorption and amine efficiency of titania modified by moderate loading of diethylenetriamine. *Journal of Material Chemistry A*. 2013;1:6208-15.
33. Xu H, Zeiger BW, Suslick KS. Sonochemical synthesis of nanomaterials. *Chemical Society reviews*. 2013;42(7):2555-67.
34. Hickenboth CR, Moore JS, White SR, Sottos NR, Baudry J, Wilson SR. Biasing Reaction Pathways with Mechanical Force. *Nature*. 2007;446:423.
35. Herrero M, Labajos FM, Rives V. Size Control and Optimisation of Intercalated Layered Double Hydroxides. *Applied Clay Science*. 2009;42:510-8.
36. Wypych F, Bail A, Halma M, Nakagaki S. Immobilization of iron(III) porphyrins on exfoliated MgAl layered double hydroxide, grafted with (3-aminopropyl)triethoxysilane. *Journal of Catalysis*. 2005;234(2):431-7.
37. Kong Y, Shen X, Cui S, Fan M. Development of monolithic adsorbent via polymeric sol-gel process for low-concentration CO<sub>2</sub> capture. *Applied Energy*. 2015;147:308-17.
38. Kong Y, Jiang G, Wu Y, Cui S, Shen X. Amine hybrid aerogel for high-efficiency CO<sub>2</sub> capture: Effect of amine loading and CO<sub>2</sub> concentration. *Chemical Engineering Journal*. 2016;306:362-8.

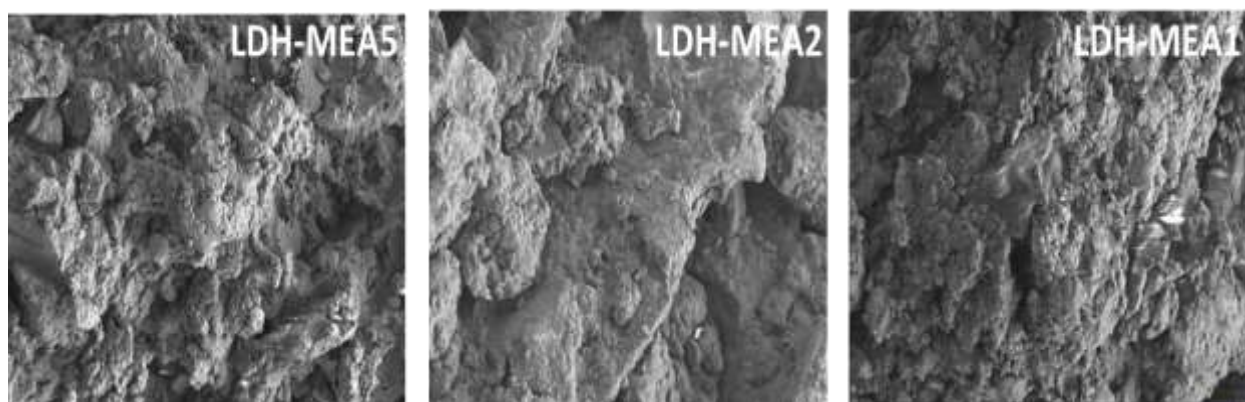
#### LIST OF FIGURES

Figures	Caption
1	SEM Images of prepared LDHs with variation in Surfactant, SDS
2	SEM images of LDH-MEAn at various APTS/SDS mole ratios (n = 5, 2 and 1)
3	SEM image of LDH prepared via ultrasonic irradiation at APTS/SDS mole ratio = 5 using ultrasonic horn (UH-LDH5)
4	XRD patterns for LDHn (n = 1, 2 and 5) samples
5	XRD patterns for UB-LDHn (n = 1, 2 and 5) samples
6	XRD patterns for UH-LDHn (n = 1, 2 and 5) samples
7	XRD patterns for LDH-MEAn (n = 2 and 5) samples
8	XRD patterns for UB-MEAn (n = 2 and 5) samples
9	Example of (a) TGA curve for CO <sub>2</sub> adsorption, (b) recoverable CO <sub>2</sub> uptake using TSA at 105 °C in N <sub>2</sub> atmosphere.
10	CO <sub>2</sub> Uptake for (a) LDHn and (b) LDH-MEAn (with n being the molar ratio of APTS to SDS)
11	Comparison of CO <sub>2</sub> uptake by samples prepared via conventional (LDHn) and ultrasonic irradiation route (UH-LDHn and UB-LDHn) at 55 °C and 80 °C.
12	Comparison of CO <sub>2</sub> uptake by samples prepared via conventional (LDHn) and ultrasonic irradiation route (ultrasonic horn, UH-LDHn and ultrasonic bath, UB-

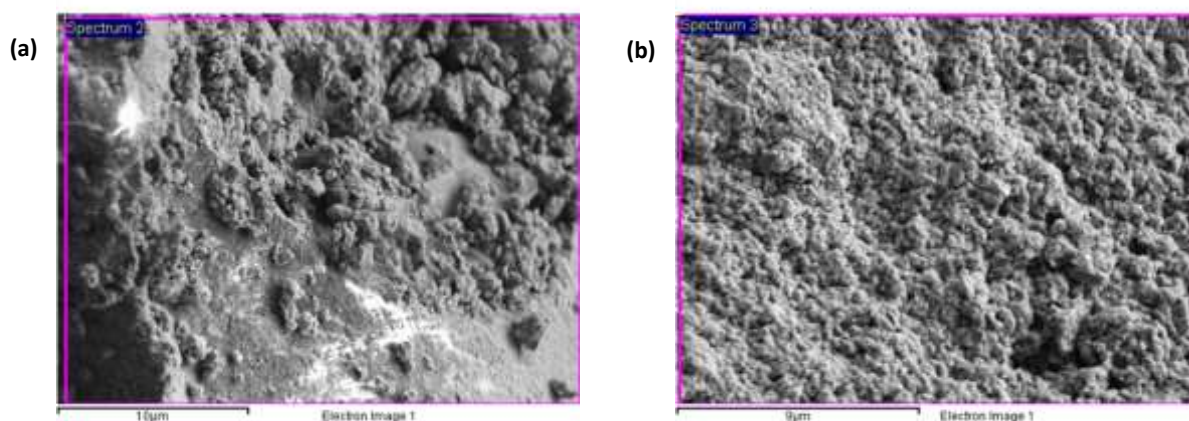
- LDHn) with APTS/SDS mole ratio,  $n = 5$  at  $55^{\circ}\text{C}$  (a) prior MEA extraction, and (b) post MEA extraction
- 13 N 1s XPS spectra for (a) LDH5 and (b) UH-LDH5
  - 14 TGA curves comparing thermal stabilities of LDHs prepared via conventional and ultrasonic irradiation: (a) LDH2, (b) UB-LDH2 and (c) UH-LDH2; as well as with amine modified LDHs: (d) LDH-MEA5 and (e) UB-MEA5 (f) UH-MEA5
  - 15 TSA Cycles of LDH-MEA5 and UH-MEA5 at  $55^{\circ}\text{C}$  (30 mins regeneration time at  $105^{\circ}\text{C}$  in  $\text{N}_2$  atmosphere) based on the initial adsorption capacity of 1.45 and 1.37 mmol/g respectively
  - 16  $\text{CO}_2$ -TPD of functionalised LDH (a) Deconvolution of the  $\text{CO}_2$ -TPD of UH-MEA5 and (b) Comparison of  $\text{CO}_2$ -TPD of UH-MEA5 and LDH-MEA5.
  - 17 Comparison of kinetic models with experimental results for  $\text{CO}_2$  uptake on (a) LDH5 and (b) UH-LDH5



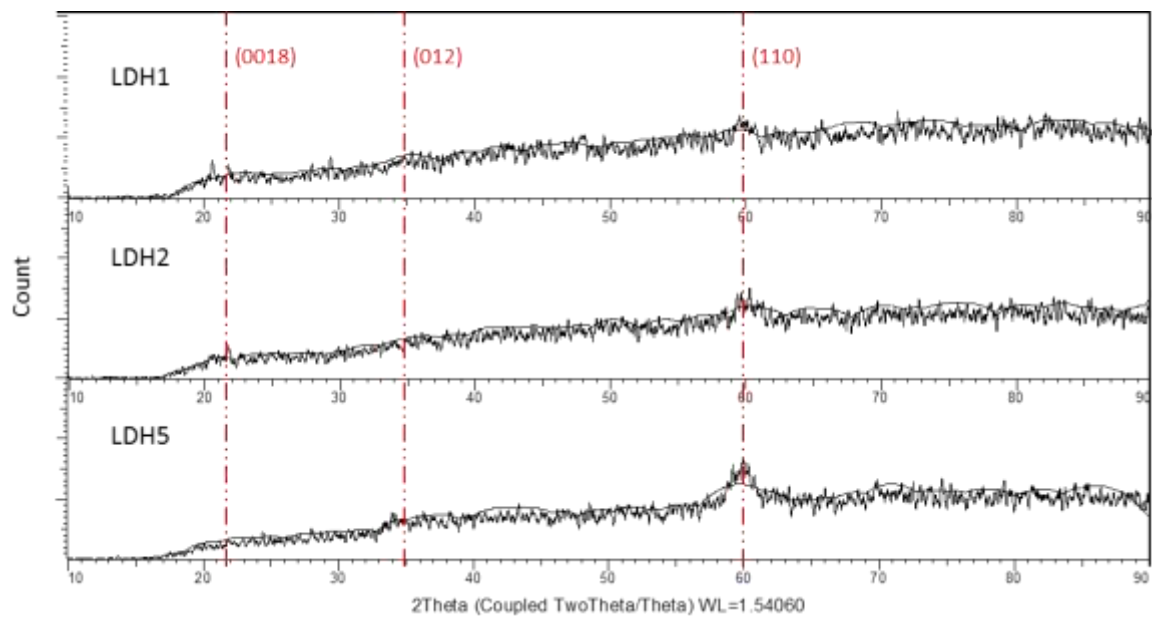
**Figure 1: SEM Images of prepared LDHs with variation in Surfactant, SDS**



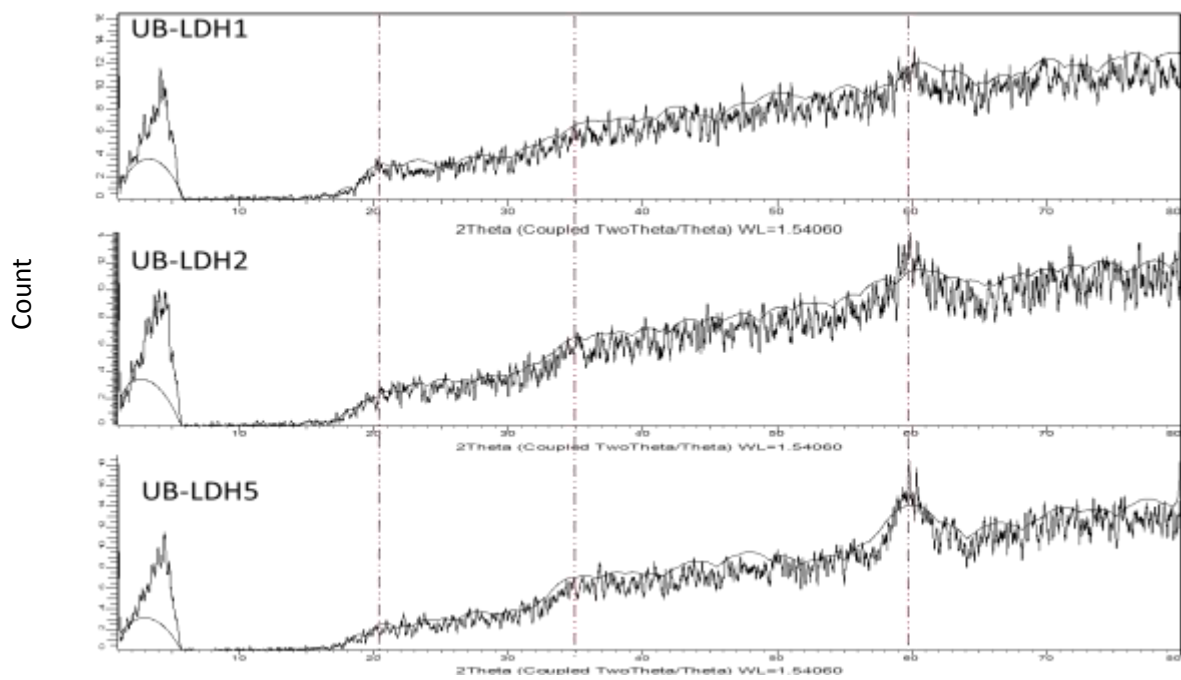
**Figure 2: SEM images of LDH-MEA<sub>n</sub> at various APTS/SDS mole ratios (n = 5, 2 and 1)**



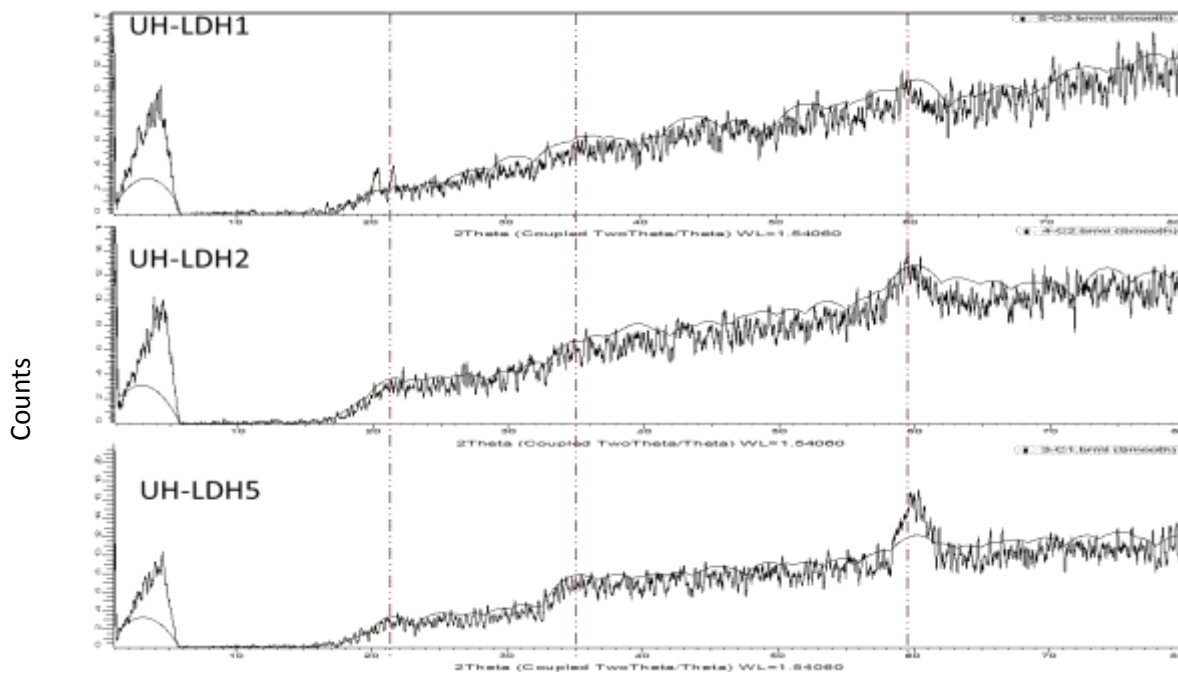
**Figure 3: Comparison of surface texture of LDH prepared via (a) conventional, and (b) ultrasonic irradiation routes, at APTS/SDS mole ratio = 5 using ultrasonic horn (UH-LDH5)**



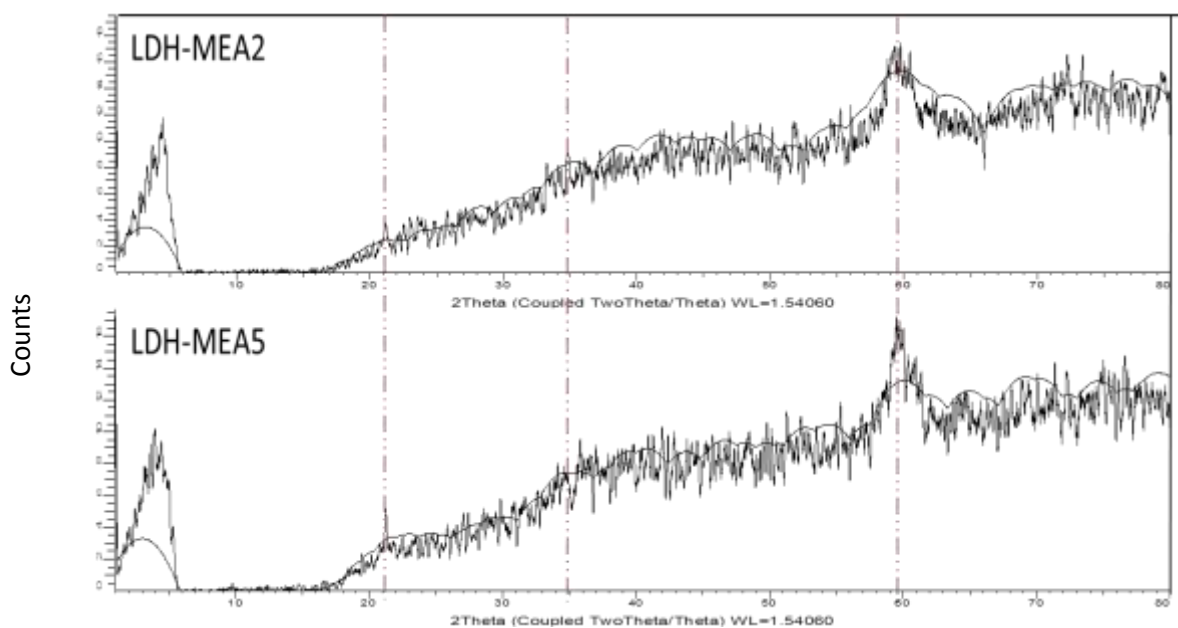
**Figure 4: XRD patterns for LDH<sub>n</sub> (n = 1, 2 and 5) samples**



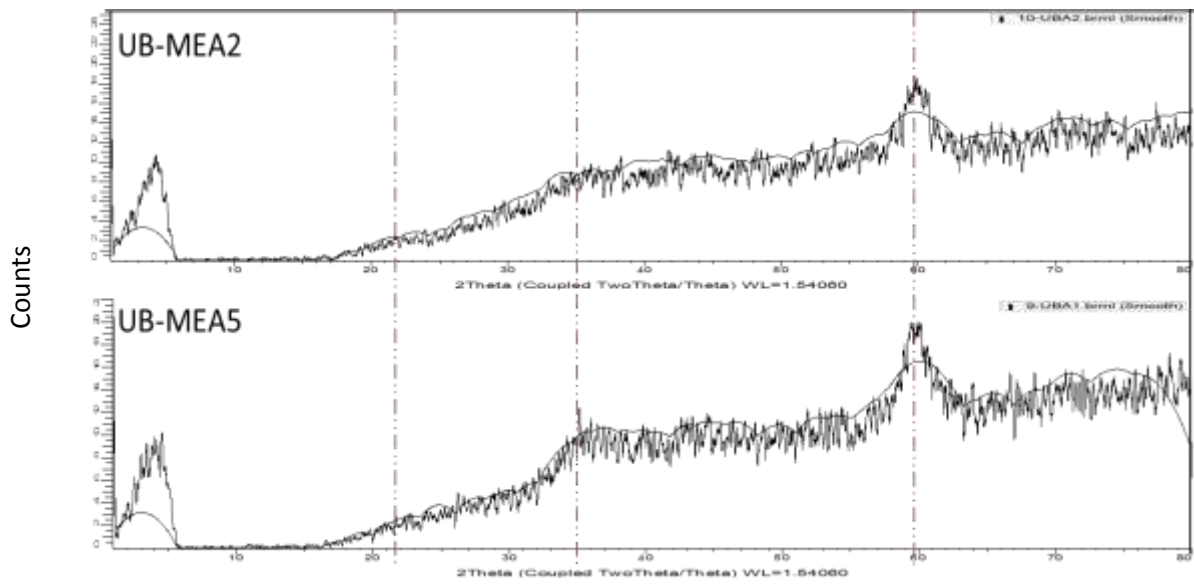
**Figure 5: XRD patterns for UB-LDH<sub>n</sub> (n = 1, 2 and 5) samples**



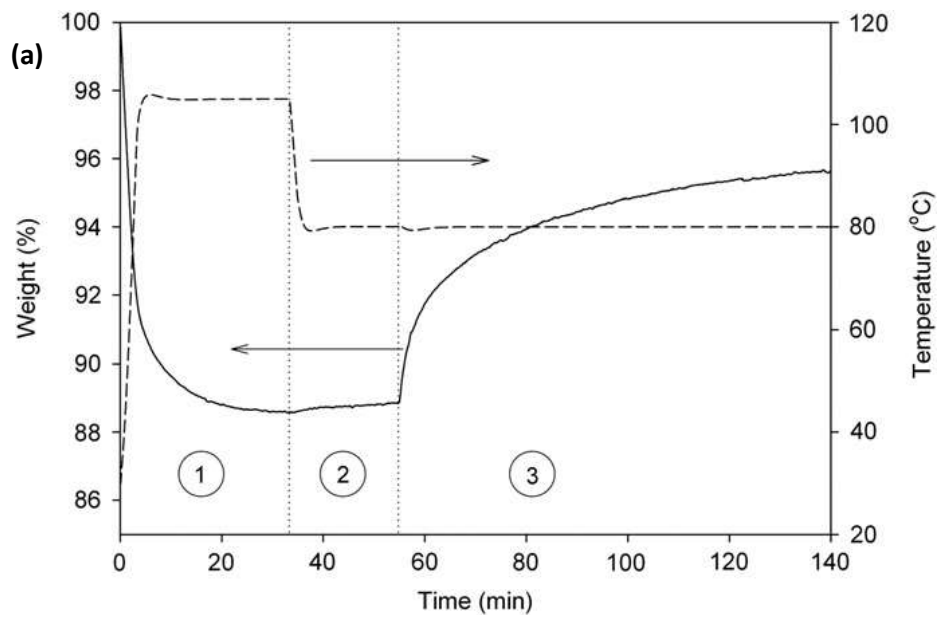
**Figure 6: XRD patterns for UH-LDH<sub>n</sub> (n = 1, 2 and 5) samples**



**Figure 7: XRD patterns for LDH-MEA<sub>n</sub> (n = 2 and 5) samples**



**Figure 8: XRD patterns for UB-MEA<sub>n</sub> (n = 2 and 5) samples**



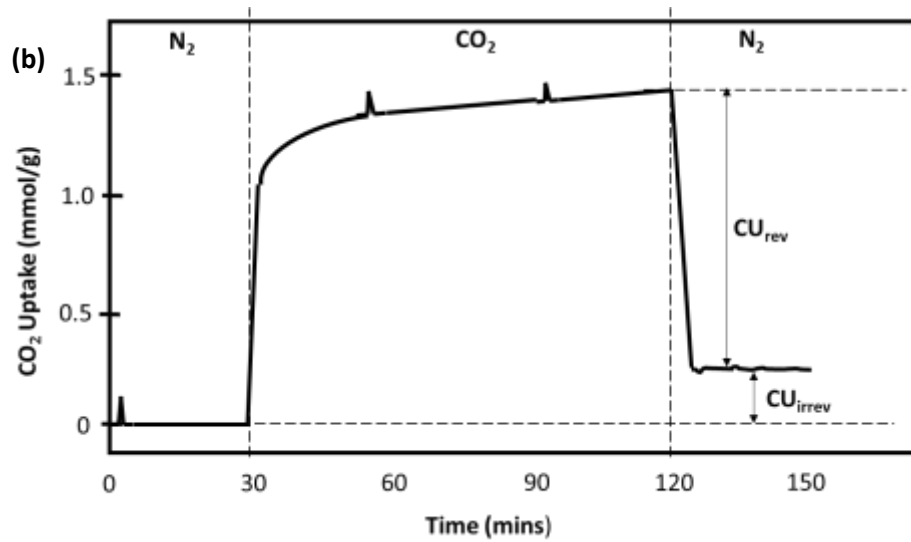
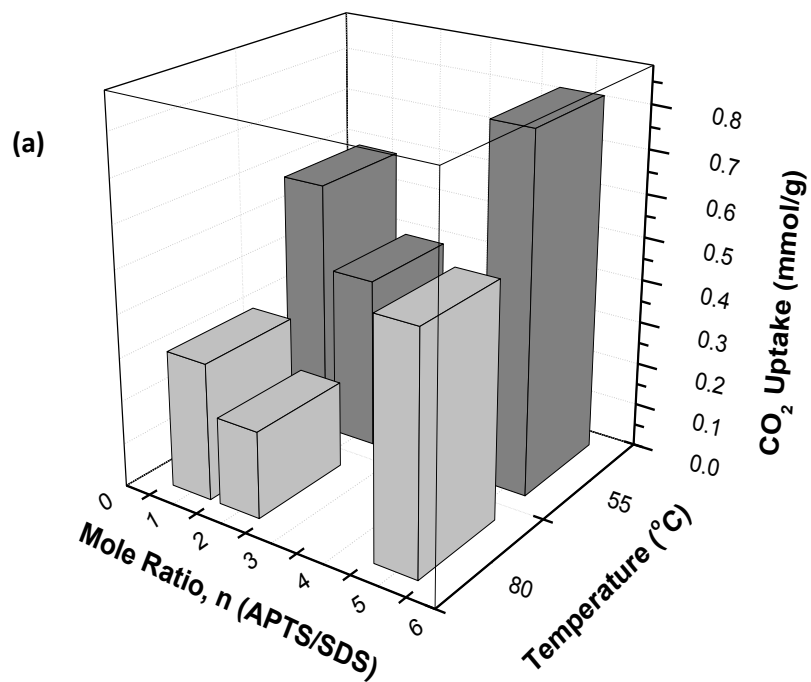


Figure 9: Example of (a) TGA curve for CO<sub>2</sub> adsorption, (b) recoverable CO<sub>2</sub> uptake using TSA at 105 °C in N<sub>2</sub> atmosphere.



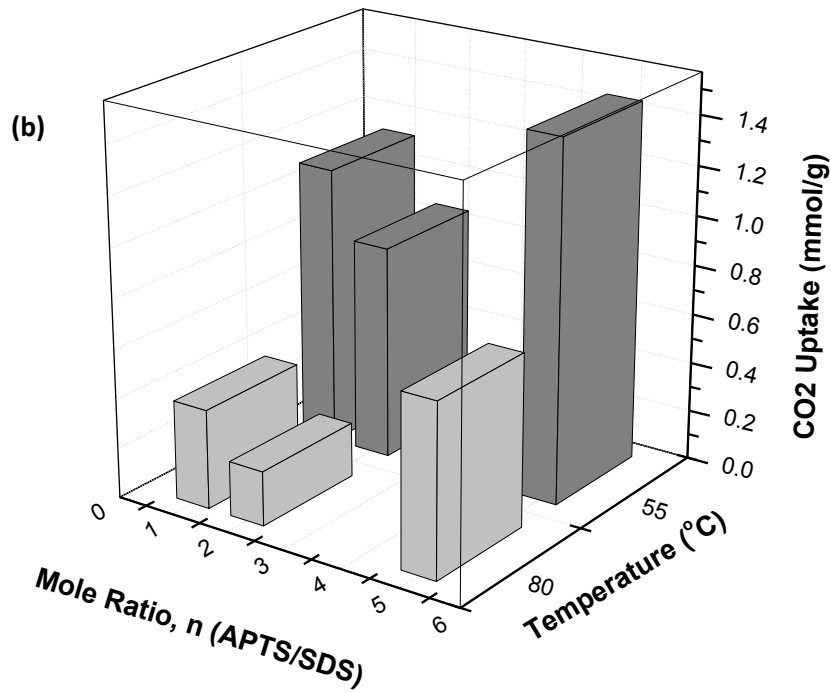


Figure 10: CO<sub>2</sub> Uptake for (a) LDHn and (b) LDH-MEAn (with n being the molar ratio of APTS to SDS)

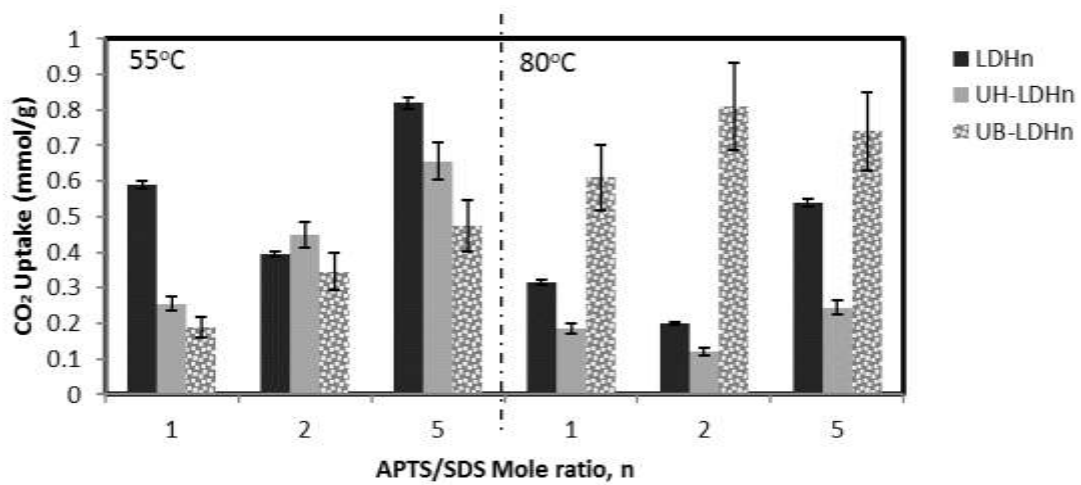
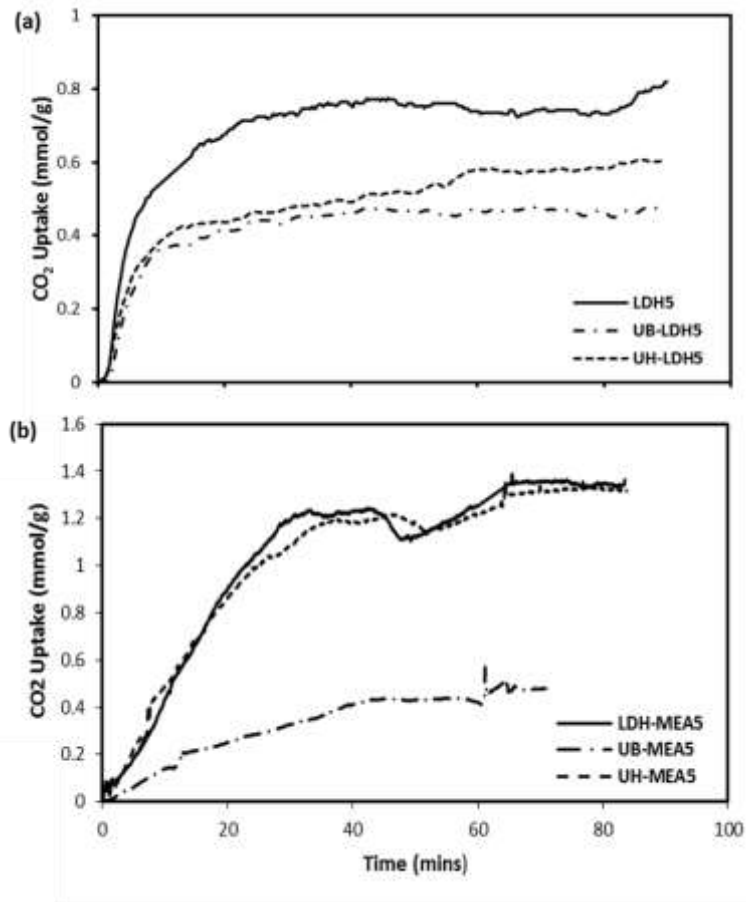
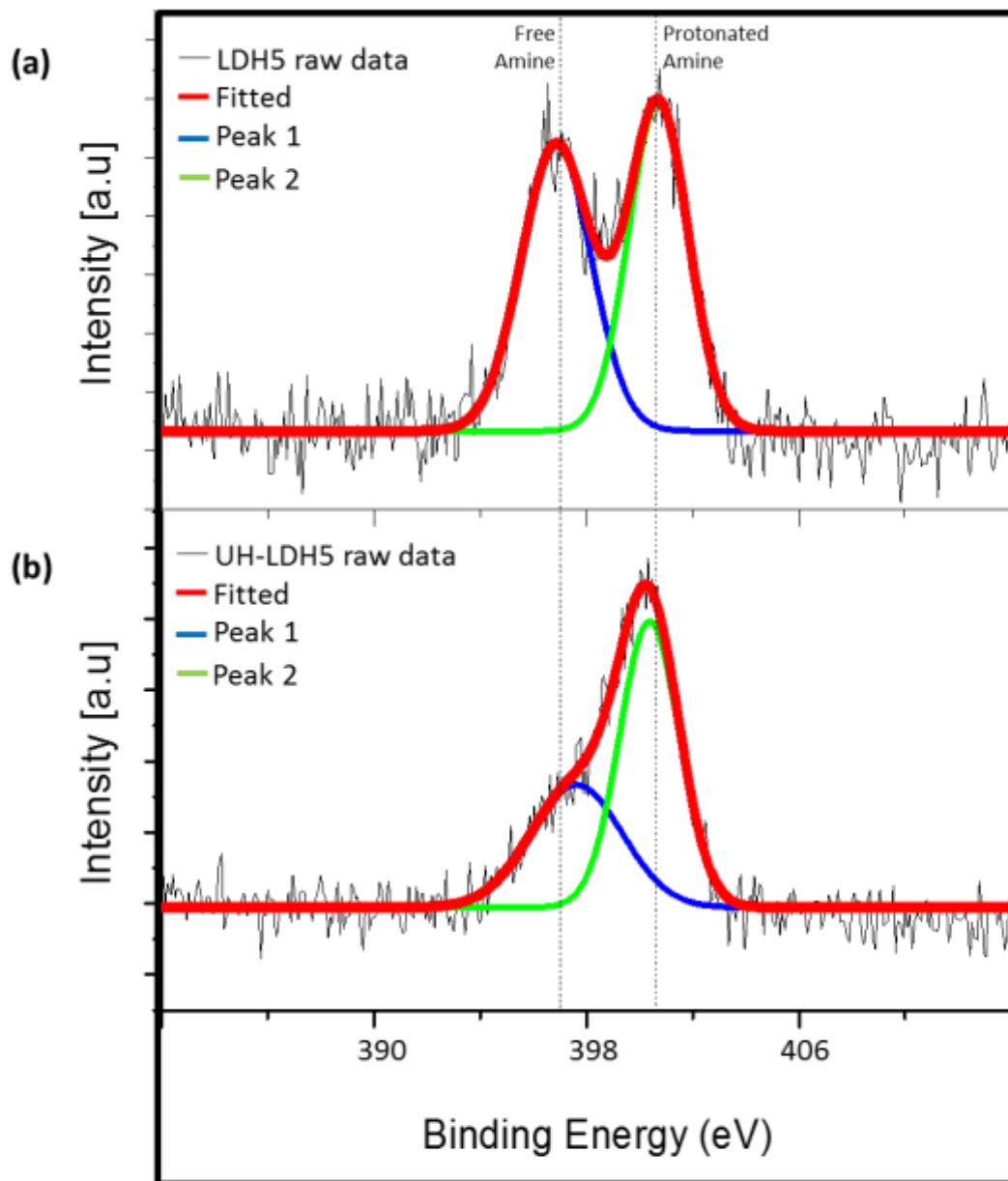


Figure 11: Comparison of CO<sub>2</sub> uptake by samples prepared via conventional (LDHn) and ultrasonic irradiation route (UH-LDHn and UB-LDHn) at 55°C and 80°C.



**Figure 12: Comparison of CO<sub>2</sub> uptake by samples prepared via conventional (LDHn) and ultrasonic irradiation route (ultrasonic horn, UH-LDHn and ultrasonic bath, UB-LDHn) with APTS/SDS mole ratio,  $n = 5$  at 55°C (a) prior MEA extraction, and (b) post MEA extraction**



Preparation Route	Sample	Binding Energy (eV)		Area (cps eV)		Content (Free/Protonated)
		Free Amine	Protonated Amine	Free Amine	Protonated Amine	
Conventional	LDH5	396.7	400.8	660.0	606.4	1.1
Sonochemical	UH-LDH5	396.9	400.3	596.0	854.7	0.7

Figure 13: N 1s XPS spectra for (a) LDH5 and (b) UH-LDH5

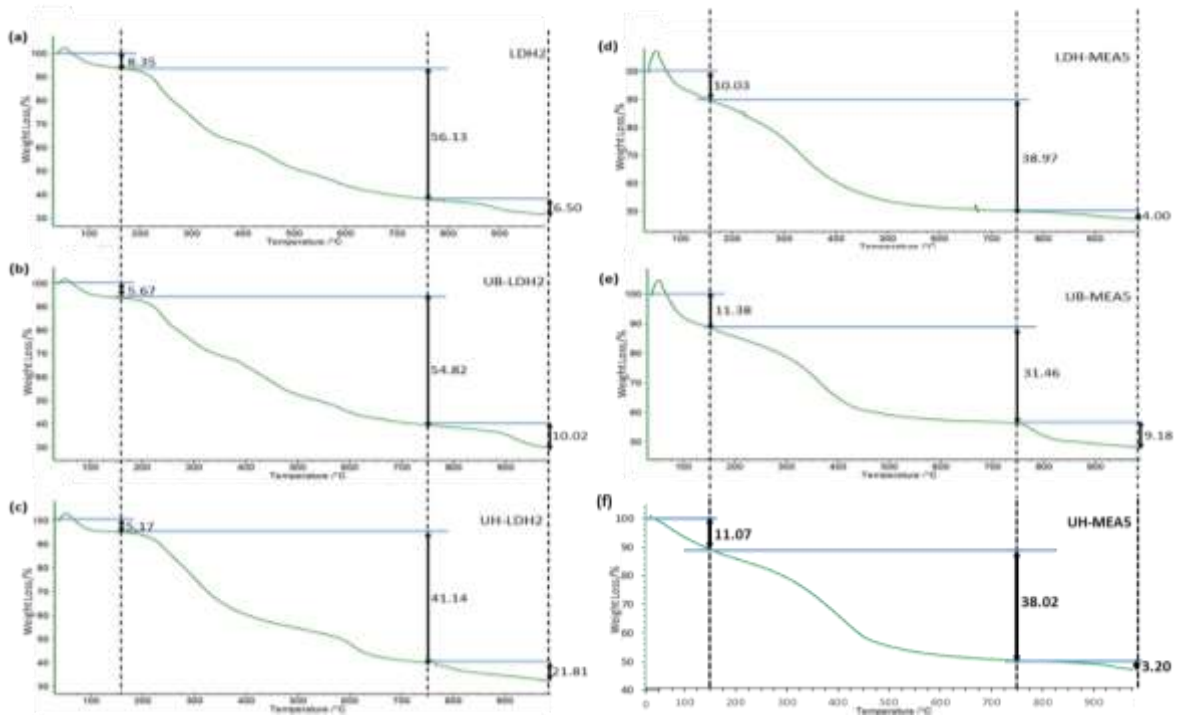


**Figure 14: TGA curves comparing thermal stabilities of LDHs prepared via conventional and ultrasonic irradiation: (a) LDH2, (b) UB-LDH2 and (c) UH-LDH2; as well as with amine modified LDHs: (d) LDH-MEA5 and (e) UB-MEA5 (f) UH-MEA5**

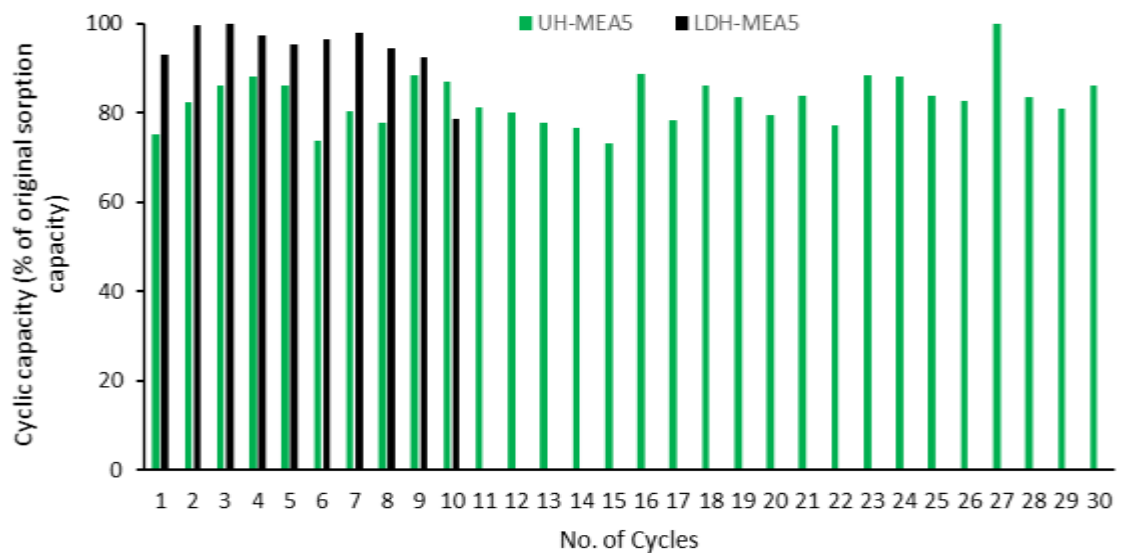


**Figure 15: TSA Cycles of LDH-MEA5 and UH-MEA5 at 55 °C (30 mins regeneration time at 105 °C in N<sub>2</sub> atmosphere) based on the initial adsorption capacity of 1.45 and 1.37 mmol/g respectively**

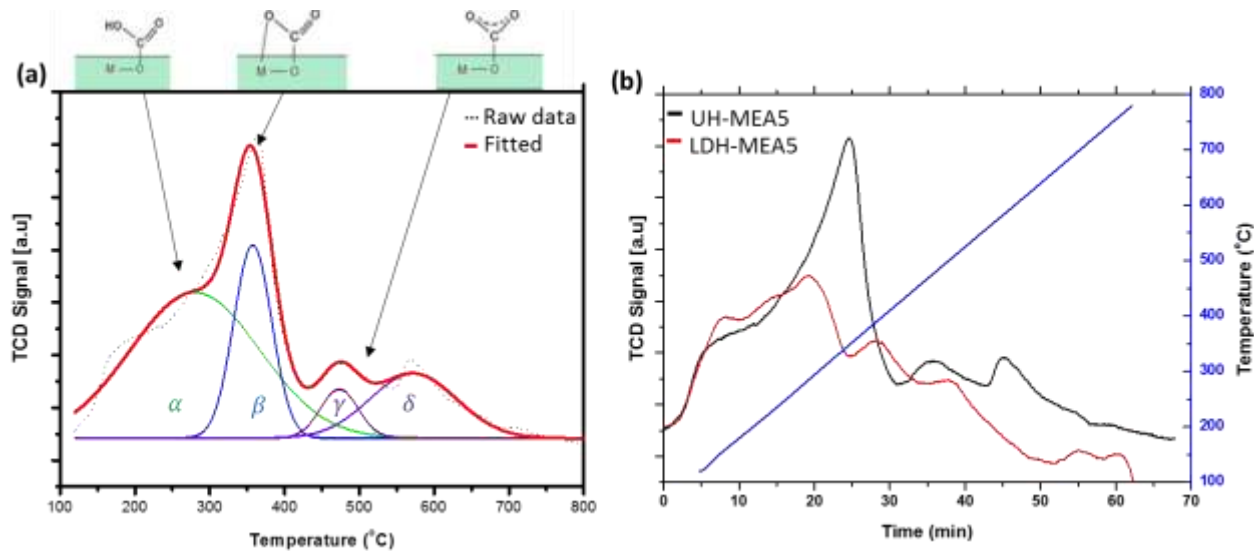


**Figure 16: CO<sub>2</sub>-TPD of functionalised LDH (a) Deconvolution of the CO<sub>2</sub>-TPD of UH-MEA5 and (b) Comparison of CO<sub>2</sub>-TPD of UH-MEA5 and LDH-MEA5.**

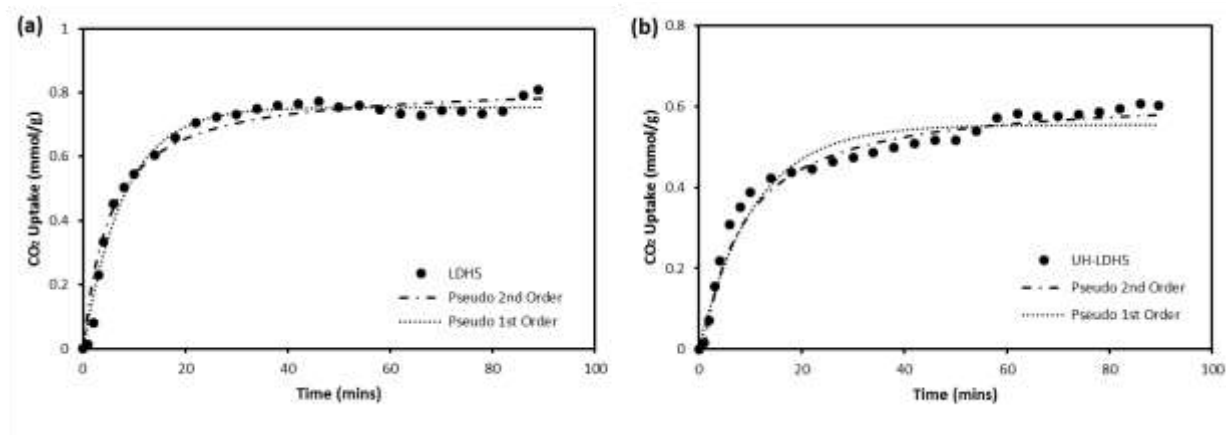


**Figure 17: Comparison of kinetic models with experimental results for CO<sub>2</sub> uptake on (a) LDH5 and (b) UH-LDH5**

## LIST OF TABLES

Tables	Caption
1	Pore structure of modified LDHs, gas uptake and recoverable adsorbed CO <sub>2</sub>
2	EDX elemental analysis and CO <sub>2</sub> uptake of prepared LDH and calculation results for the molecular formulas, removed SDS and effective amine efficiency
3	Average CO <sub>2</sub> adsorption for prepared ultrasonic mediated LDHn samples
4	Thermal degradation of samples prepared via conventional (LDHn) and ultrasonic irradiation route (UH-LDHn and UB-LDHn)
5	CO <sub>2</sub> kinetic model parameters, R <sup>2</sup> and standard errors (%) for prepared LDHs and amine functionalized LDHs at 55 °C and APTS/SDS ratio, n of 5



**Table 1: Pore structure of modified LDHs, gas uptake and recoverable adsorbed CO<sub>2</sub>**

Sample	Gas Uptake (mmol/g)		mmol N <sub>2</sub> mmol CO <sub>2</sub>	CU <sub>rev</sub>	CU <sub>irrev</sub>	% of CU <sub>irrev</sub>	S <sub>BET</sub> (m <sup>2</sup> /g)	Average Pore Width (nm)	V <sub>Total</sub> (cm <sup>3</sup> /g)	V <sub>micro</sub> (cm <sup>3</sup> /g)
	CO <sub>2</sub>	N <sub>2</sub>								
LDH-MEA5	1.45	0.23	0.16	1.27	0.18	12.64	25.03	2.57	0.0161	0.0008
UB-MEA5	0.54	0.14	0.25	0.51	0.03	6.39	-	-	-	-
UH-MEA5	1.37	0.43	0.31	1.33	0.03	2.43	171.20	12.92	0.5528	0.0229

**Table 2: EDX elemental analysis and CO<sub>2</sub> uptake of prepared LDH and calculation results for the molecular formulas, removed SDS and effective amine efficiency**

Sample	N (wt%)	C (wt%)	S (wt%)	Molecular formula (mmol/g) <sup>a</sup>	SDS/APTS	Amine Loading (mmol/g)	CO <sub>2</sub> Adsorbed (mmol/g)	SDS removed (%)	Effective amine loading (mmol/g) <sup>b</sup>	Effective Amine Efficiency <sup>c</sup>
LDH5	0.65	51.35	11.41	[C <sub>12</sub> H <sub>25</sub> SO <sub>4</sub> ] <sub>3.57</sub> ·[C <sub>0.01</sub> H <sub>0.52</sub> SiNO <sub>3</sub> ] <sub>0.46</sub>	7.68	0.46	0.82			
LDH-MEA5	6.60	26.60	1.05	[C <sub>12</sub> H <sub>25</sub> SO <sub>4</sub> ] <sub>0.33</sub> ·[C <sub>3.87</sub> H <sub>10.17</sub> SiNO <sub>3</sub> ] <sub>4.71</sub>	0.07	4.71	1.45	99.09	4.25	0.15
UB-LDH5	1.69	47.78	8.22	[C <sub>12</sub> H <sub>25</sub> SO <sub>4</sub> ] <sub>2.57</sub> ·[C <sub>7.45</sub> H <sub>19.12</sub> SiNO <sub>3</sub> ] <sub>1.21</sub>	2.13	1.21	0.48			
UB-MEA5	7.37	25.38	0.64	[C <sub>12</sub> H <sub>25</sub> SO <sub>4</sub> ] <sub>0.20</sub> ·[C <sub>3.56</sub> H <sub>9.40</sub> SiNO <sub>3</sub> ] <sub>5.26</sub>	0.04	5.26	0.54	98.21	4.06	0.02
UH-LDH5	3.11	51.16	11.08	[C <sub>12</sub> H <sub>25</sub> SO <sub>4</sub> ] <sub>3.46</sub> ·[C <sub>0.49</sub> H <sub>1.72</sub> SiNO <sub>3</sub> ] <sub>2.22</sub>	1.56	2.22	0.66			
UH-MEA5	7.34	30.64	0.60	[C <sub>12</sub> H <sub>25</sub> SO <sub>4</sub> ] <sub>0.19</sub> ·[C <sub>4.44</sub> H <sub>11.60</sub> SiNO <sub>3</sub> ] <sub>5.24</sub>	0.04	5.24	1.37	97.71	3.02	0.24

a All Nitrogen, Carbon and Sulphur elements in the grafted LDHs were attributed to come from organic compounds used for intercalation

b. Effective amine loading = Difference in amine loading before and after LDH modification

c. Effective Amine Efficiency = Difference in CO<sub>2</sub> adsorbed before and after LDH modification/effective amine loading

**Table 3: Average CO<sub>2</sub> adsorption for prepared ultrasonic mediated LDHn samples**

Sample		UH-LDH5	UH-LDH2	UH-LDH1	UB-LDH5	UB-LDH2	UB-LDH1
55°C	1st Trial	0.70	0.39	0.21	0.49	0.34	0.21
	2nd Trial	0.61	0.51	0.30	0.46	0.35	0.17
	<b>Average</b>	<b>0.655</b>	<b>0.45</b>	<b>0.255</b>	<b>0.475</b>	<b>0.345</b>	<b>0.19</b>
80°C	1st Trial	0.21	0.09	0.13	0.74	0.81	0.61
	2nd Trial	0.28	0.15	0.24	-	-	-
	<b>Average</b>	<b>0.245</b>	<b>0.12</b>	<b>0.185</b>	<b>0.74</b>	<b>0.81</b>	<b>0.61</b>

**Table 4: Thermal degradation of samples prepared via conventional (LDHn) and ultrasonic irradiation route (UH-LDHn and UB-LDHn)**

Preparation Route	APTS/SDS mole ratio, n	Sample Name	Weight Loss (%)			
			T<150°C	150< T<750°C	750°C< T	Total
Conventional	5	LDH5	10.43	43.63	11.24	<b>65.30</b>
	2	LDH2	8.35	56.13	6.50	<b>70.98</b>
	1	LDH1	2.73	46.02	20.30	<b>69.05</b>
Ultrasonic Bath	5	UB-LDH5	9.36	46.63	8.76	<b>64.75</b>
	2	UB-LDH2	5.67	54.82	10.02	<b>70.51</b>
	1	UB-LDH1	5.05	57.95	8.39	<b>71.39</b>
Ultrasonic Horn	5	UH-LDH5	9.04	44.74	12.39	<b>66.17</b>
	2	UH-LDH2	5.17	41.14	21.81	<b>68.12</b>
	1	UH-LDH1	3.77	36.32	13.46	<b>53.55</b>

**Table 5: CO<sub>2</sub> kinetic model parameters, R<sup>2</sup> and standard errors (%) for prepared LDHs and amine functionalized LDHs at 55 °C and APTS/SDS ratio, n of 5**

Samples	Pseudo 2nd Order		Err (%)	R <sup>2</sup>	Pseudo 1st Order		Err (%)	R <sup>2</sup>
	A <sub>2</sub>	k <sub>2</sub>			A <sub>1</sub>	k <sub>1</sub>		
LDH5	0.83		0.22	0.9483	0.76		0.23	0.9281
UB-LDH5	0.51	0.05	0.54	0.9609	0.46	0.06	0.38	0.9292
UH-LDH5	0.63		0.84	0.9629	0.56		0.74	0.9057
LDH-MEA5	1.35		0.16	0.8306	1.38		0.20	0.8177
UB-MEA5	0.51	0.04	0.13	0.8583	0.45	0.03	0.13	0.8361
UH-MEA5	1.67		0.55	0.8909	1.32		0.20	0.9226